0014-4754/96/080778-08$1.50 + 0.20

Induction of vanadium accumulation and nuclear sequestration causing cell suicide in human Chang liver cells

K. H. Sit[a,*], R. Paramanantham[a], B. H. Bay[a], K. P. Wong[b], P. Thong[c] and F. Watt[c]

[a] *Department of Anatomy, National University of Singapore, Kent Ridge 0511 (Singapore), Fax +65 7787 643*
[b] *Department of Biochemistry, National University of Singapore, Kent Ridge 0511 (Singapore)*
[c] *Department of Physics, National University of Singapore, Kent Ridge 0511 (Singapore)*
Received 5 October 1995; received after revision 30 January 1996; accepted 5 March 1996

Abstract. Very little is known about the modulation of vanadium accumulation in cells, although this ultratrace element has long been seen as an essential nutrient in lower life forms, but not necessarily in humans where factors modulating cellular uptake of vanadium seem unclear. Using nuclear microscopy, which is capable of the direct evaluation of free and bound (total) elemental concentrations of single cells we show here that an NH_4Cl acidification prepulse causes distinctive accumulation of vanadium (free and bound) in human Chang liver cells, concentrating particularly in the nucleus. Vanadium loaded with acidification but leaked away with realkalinization, suggests proton-dependent loading. Vanadyl(4), the oxidative state of intracellular vanadium ions, is known to be a potent source of hydroxyl free radicals ($OH^{\bullet}$). The high oxidative state of nuclei after induction of vanadyl(4) loading was shown by the redox indicator methylene blue, suggesting direct oxidative damage to nuclear DNA. Flow cytometric evaluation of cell cycle phase-specific DNA composition showed degradation of both 2N and 4N DNA phases in G_1, S and G_2/M cell cycle profiles to a solitary 1N DNA peak, in a dose-dependent manner, effective from micromolar vanadyl(4) levels. This trend was reproduced with micrococcal nuclease digestion in a time response, supporting the notion of DNA fragmentation effects. Several other approaches confirmed fragmentation occurring in virtually all cells after 4 mM V(4) loading. Ultrastructural profiles showed various stages of autophagic autodigestion and well defined plasma membrane outlines, consistent with programmed cell death but not with necrotic cell death. Direct intranuclear oxidative damage seemed associated with the induction of mass suicide in these human Chang liver cells following vanadium loading and nuclear sequestration.

Key words. Quantitation of intracellular vanadium (free and bound); nuclear sequestration of vanadium; nuclear microscopy; cell cycle phase-specific evaluation of sub-2N DNA in flow cytometry; programmed cell death; autophagic autodigestion.

Vanadium ions are regarded as trace components of mammalian cells where they occur in the bioreduced vanadyl(4) oxidative state[1]. They are thought to have mitogenic potential[2] as well as significant regulatory and therapeutic functions, such as inhibition of transmembrane export pumps in the modulation of cytosolic acidification[3] and inhibition of ATP-dependent glutathione S-conjugate export[4,5], inhibition of phosphotyrosine phosphatase producing insulin mimetic effects[6], and cancer chemopreventive efficacies[7,8]. However, the knowledge of basic metabolic processes regulating vanadium is cited as incomplete[9], notwithstanding calls for upgrading the uptake of this trace element to essential nutrient status in humans[10]. Using nuclear microscopy that incorporates (a) particle-induced X-ray emission (PIXE) to measure directly total (free and bound) elemental concentrations in single cells, (b) Rutherford backscattering spectrometry (RBS) which provides information on the matrix elements C, N and O, and (c) scanning transmission ion microscopy (STIM) which provides information on the structure and density of the cell and its nucleus through transmitted proton energy loss[11–14], we show here that cellular acidification induces massive accumulation of vanadium (free and bound) ions in the nucleus. Since vanadyl(4) itself induces cellular acidification[3] that is needed for its entry, cellular loading appears self-serving, once initiated, especially in proton-translocating and acid-secreting cells in the stomach, kidney and urinary bladder, acid-secreting osteoclasts and phagocytes.

Vanadyl(4) ions generate hydroxyl free radicals ($OH^{\bullet}$) and cause lipid peroxidation[15–18], factors that have recently been implicated in causing cell suicide or apoptosis/programmed cell death[19–22]. On the other hand, vanadium toxicity has previously been associated with necrosis in a number of tissue systems[23–25]. Here we show features consistent with programmed cell death.

* Corresponding author.

Materials and methods

Monolayer cultures of human Chang liver cells (ATCC CCL 13) were grown in Dulbecco's modified Eagle's medium (DMEM, Sigma) with 10% fetal calf serum (Biological Industries, Israel). Parallel cultures were seeded in 25 cm^2 flasks (Costar) at 3×10^5 cells/flask from stirred stock suspension and grown to near confluency.

For nuclear microscopy, cultures were seeded on serum-prepulsed Pioloform film anchored by Permount over an aluminium target holder and processed as previously described[11]. For measurement of intracellular pH (pH_i), the cells were loaded with 10 μM BCECF-am (Molecular Probes) using the detailed protocol previously described[26]. The acidification buffer was NH_4Cl (50 mM NH_4Cl, 50 mM glucose) with or without addition of 4 mM vanadium(IV) oxide sulphate pentahydrate (vanadyl(4), Fluka) which was prepared by dissolving first in H_2O and adjusted to pH 5.5 using 4N NaOH (the unadjusted vanadyl(4) solution contained the oxovanadium V(4) ion with a pH of 2.5 and was bright blue in colour). The pH adjustment caused a dark grey precipitation that redissolved an hour later to form a black solution of pH 4.5. The control acidification buffer without V(4) was also adjusted to pH 4.5 to match that of the experimental acidification buffer. This unshaken black solution is fairly stable (with shaking and exposure to air, however, the black vanadyl(4) solution becomes readily oxidized to dark green and finally yellow, the colour of the dioxovanadium V(5) ion). NH_4Cl and glucose were added to the black vanadyl(4) solution. The control recovery buffer was normal DMEM culture medium containing 10% foetal bovine serum (DMEM10). The experimental recovery buffer contained in addition 4 mM vanadyl(4). Cells were given a 30 min prepulse (37 °C) in NH_4Cl (with and without vanadyl(4)), and then 2 h of recovery (37 °C) in DMEM10 (with and without vanadyl(4)). Dose-responses were conducted with 40 μM to 4 mM vanadyl(4) concentrations. The incubated cell suspension was evaluated for propidium iodide (PI) binding to DNA in cell cycle phase-specific analysis, as well as for BCECF fluorescence ratio in pH analysis, using the Epics Profile II flow cytometer as previously described[3,27]. Micrococcal nuclease (Worthington Diagnostics, Flow-General, USA) digestion of fixed control cell samples was done using 80 units of the DNase in 1 ml of the cell suspension in complete Dulbecco's phosphate buffered saline (PBS complete with Ca^{2+}, Mg^{2+} complement, pH 7.4). All control and experimental cell samples were similarly fixed in 1% Bouin's fluid in PBS. DNA fragmentation induced by vanadyl(4) treatment was evaluated by terminal deoxynucleotidyl transferase (TdT)-mediated d-UTP labelling of 3'OH DNA nicks (ApopTag from Oncor, USA) in the Coulter Epics II flow cytometer. The manufacturer's protocol was followed. Hydroxyl free radicals readily form 2-hydroxybenzoates with directly added benzoic acid and produce a specific fluorescence at the excitation/emission wavelengths of 304/413 nm[28]. We used the Spex Fluoromax photon counting fluorometer to evaluate OH'-benzoic adducts in vanadyl(4) at pH 4 and 7.

The oxidative reactivity of human Chang liver cells after vanadium loading was tested using the redox indicator, methylene blue, which becomes metachromatic when oxidized but colourless in the reduced state. After 30 min NH_4Cl acidification prepulse and 15 min recovery in normal DMEM, the cells were fixed in 100% methanol for 3 min, and then stained for 3 min in 3 ml aqueous methylene blue (0.5 mg/ml) and air dried.

Cellular content of glutathione (GSH), the main reducing agent in cells, was evaluated by GSH-monochlorobimane (Molecular Probes, Oregon) adduct fluorescence in the Reichert Univar incident-light fluorescence microscope. Protocol and monochlorobimane concentration used was as previously described[19].

Results and discussion

Figure 1A shows that incubating human Chang liver cells in the NH_4Cl buffer (pH 4.5) with and without vanadyl(4) ions had caused intracellular acidification, evaluated cell-by-cell in flow cytometry using the proton chelator BCECF in ratiometric analysis. The acidification response was greater in the presence of vanadyl(4), viz. intracellular pH (pH_i) was 4.2 when incubated with vanadyl(4) (fig. 1A, thick solid line), against 5.2 when incubated without vanadyl(4) (fig. 1A, dotted line), an effect we have previously noted[3]. However, both recovered in normal DMEM after the acidification prepulse, to the resting pH 7 level. With the acidification prepulse, quantitation of particle-induced X-ray emission (PIXE) spectral energies in nuclear microscopy showed intense loading of vanadium (free and bound) into the human Chang liver cells, i.e. 56,922 ppm of dry weight above the control ultratrace level or a differential rise of 1.1174 Eq per kg dry weight (figs 1B, 2B). Bitmapping of PIXE energy revealed a strong concentration in the centre of the cell, corresponding to the nuclear area defined by simultaneous scanning transmission ion microscopy (STIM) (fig. 3B, cf. 3A). Vanadyl(4) loading occurred concomitantly with prepulse acidification and declined as dramatically with pH recovery, suggesting proton-dependent fluxes. Since vanadyl(4) induces cellular acidification, vanadyl-loading becomes an incremental self-serving cycle.

Cell cycle phase-specific DNA studies in a dose-response from 40 μM to 4 mM vanadyl(4) concentrations, evaluated by flow cytometry (fig. 4A), showed increasing degradation of 4N and 2N DNA in the G_1, S and G_2/M phases. They were eventually replaced by a

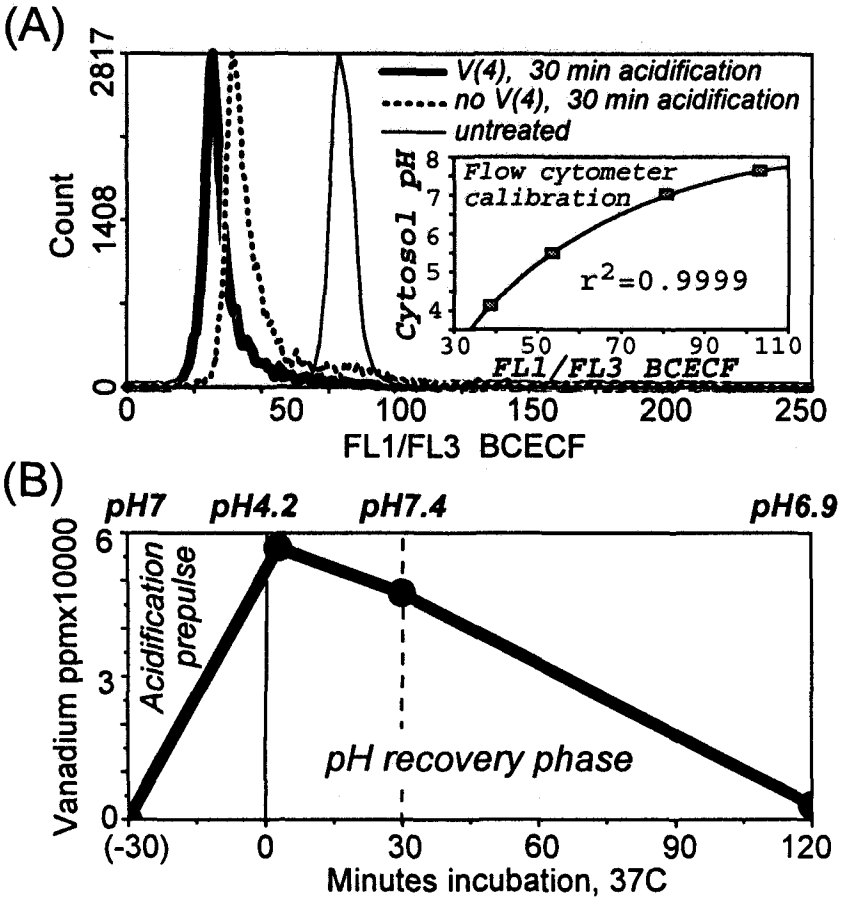

Figure 1. (*A*) Flow cytometric cell-by-cell evaluation of intracellular pH (cytosolic BCECF ratios) in human Chang liver cells incubated in 50 mM NH_4Cl-glucose for 30 min, with (thick line) and without (dotted line) 4 mM vanadyl(4) or V(4) ions. Acidification was more intense in the presence of V(4). However, both realkalinized to physiological levels with subsequent recovery incubation in normal culture medium (DMEM). (*B*) Vanadium (free and bound) concentration in human Chang liver cells in the acidification-and-recovery cycle depicted in (*A*), evaluated by particle induced X-ray emission (PIXE, in nuclear microscopy). With acidification, the total vanadium concentration in the Chang cells reached 56,922 (±4,807) ppm, way above the ultratrace level before incubation. In the cytosolic pH recovery phase, vanadium concentration dropped to 47,497 (±3,071) ppm after 30 min when pH_i was 7.4, despite the continuing presence of 4 mM vanadyl(4) in the DMEM recovery medium. By 120 min, the total (free and bound) vanadium concentration was only 3,075 (±105) ppm. Vanadium accumulated intensely with acidification, and levels fell as dramatically with pH recovery.

solitary peak of sub-2N DNA (left shifted sub-G_1 in position, fig. 4A[iv]) indicating fragmentation of genomic DNA resembling the sub-2N DNA profile seen in programmed cell death in these human Chang liver cells when deprived of serum growth factors[27] and in cells induced into programmed cell death by glucocorticoid treatment[29], and γ-irradiation[30]. Cells in necrotic cell death should have cell cycle profiles showing accumulation of 2N DNA in the G_0/G_1 phase[31] rather than accumulation of sub-2N DNA which is characteristic of programmed cell death. DNA fragmentation from applied micrococcal nuclease digestion (80 units) produced a similar left-shift of the DNA profiles in a time-course from 10 to 60 min reproducing the solitary sub-2N DNA peak of fig. 4A(iv) (see fig. 4B). Terminal deoxynucleotidyl transferase (TdT)-mediated labelling of 3′OH ends of fragmented DNA in vanadyl(4)-treated cells further confirmed the occurrence of rapid DNA degradation, affecting virtually every cell in the population (fig. 4C). Forward- and side-scatter bitmaps in flow cytometry showed significant downsizing of cells and increase in granularity, respectively, showing rapid cell condensation occurring concomitantly with DNA fragmentation which are both hallmarks of programmed cell death. Cell necrosis would have osmotic lysis which is characterized by swelling, not condensation.

Hydroxyl free radicals (OH•) generated by vanadyl(4) were assessed using spectrofluorometric evaluation of OH•-benzoic adducts that fluoresced specifically at 304/413 nm[28]. OH• appeared to be generated at pH 7 rather than at pH 4 (fig. 5) suggesting that a burst of OH• free radicals could be triggered with pH_i recovery, imposing an immediate state of oxidative stress in the nuclear

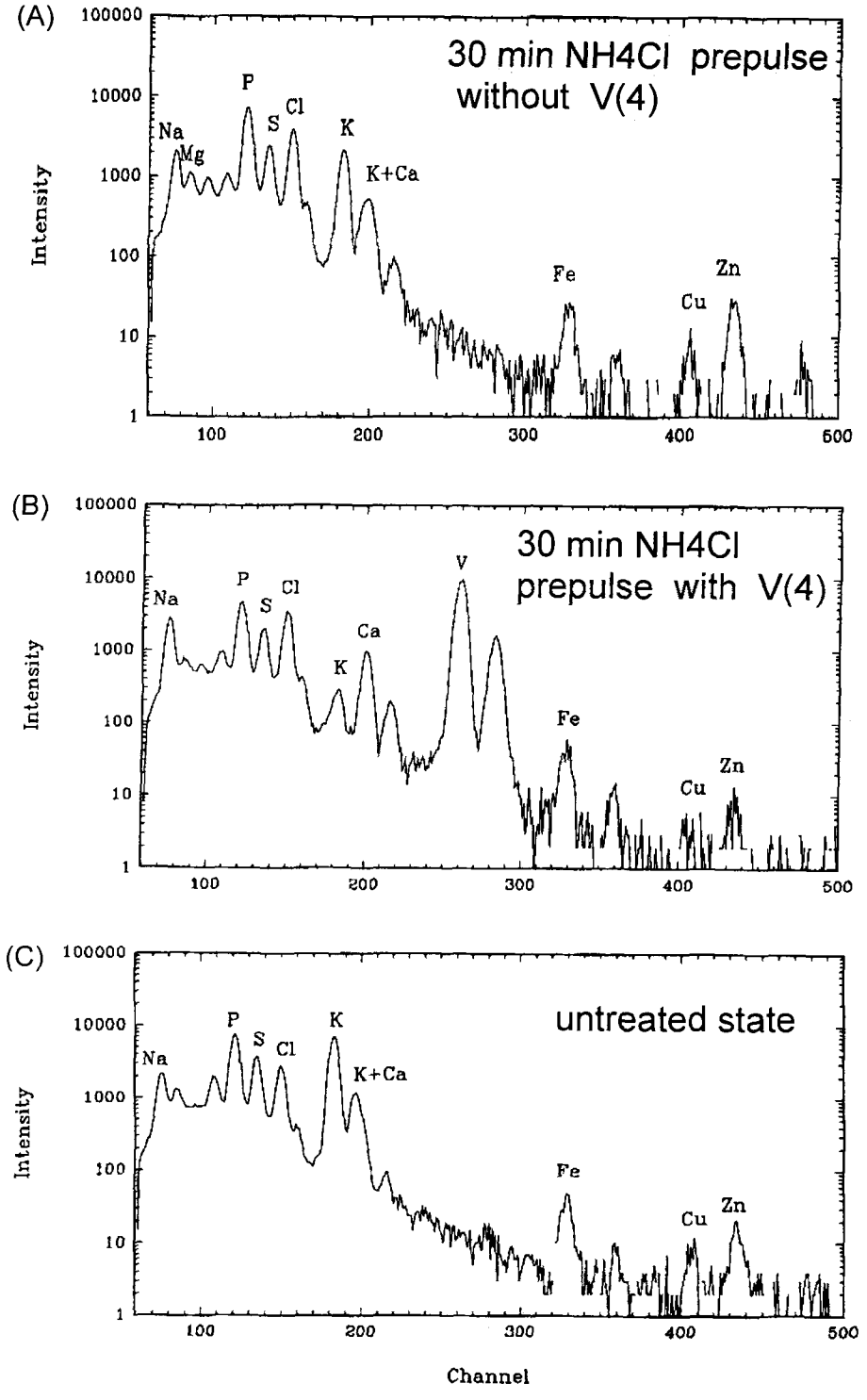

Figure 2. Particle induced X-ray emission (PIXE) elemental spectra of human Chang liver cells. (*A*) 30 min NH_4Cl-induced acidification prepulse incubation without vanadyl(4): no vanadium peak. (*B*) 30 min NH_4Cl-induced acidification prepulse incubation containing 4 mM vanadyl(4): massive vanadium loading, indicated by the tall vanadium (V) peak in the log scale. (*C*) Untreated resting counterpart: no vanadium peak. Here the K^+ peak is clearly higher than the Na^+ peak, giving a high K^+/Na^+ ratio. With V(4) treatment, there is precipitous K^+ loss but significant Na^+ gain, resulting in a reversal of the K^+/Na^+ ratio.

compartment. The OH^- burst coincided with a dramatic reversal of the total (free and bound) K^+/Na^+ ratio immediately after the acidification prepulse. Three minutes into the recovery phase, the K^+/Na^+ ratio dropped from 15.65:1 to 0.13:1. Na^+ concentration increased by 472%, rising from 3,980 ppm dry wt ($\pm$166) to 18,799 ppm dry wt ($\pm$545), while K^+ concentration decreased to a mere 4% of its original

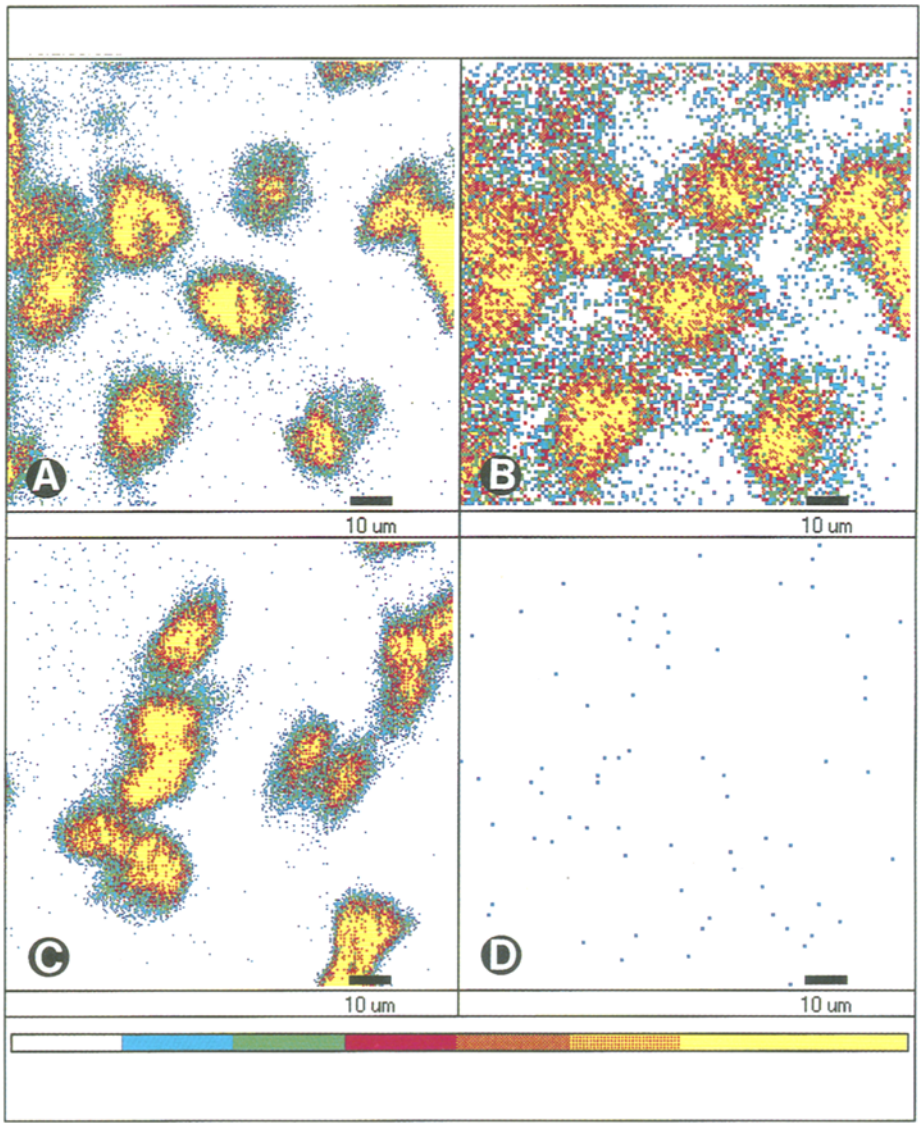

Figure 3. Localization of vanadium loading using bitmapping in scanning transmission ion microscopy (STIM) and particle induced X-ray emission (PIXE) quantitation in nuclear microscopy. (*A*) STIM bitmap of vanadyl(4)-prepulsed human Chang liver cells (cells of fig. 2B) showing cell profiles and the nuclear area which is more dense and coloured yellow (yellow indicates the highest intensity in the pseudocolour scale from white (low end) to yellow (high end) shown at the bottom of the figure). (*B*) PIXE bitmap of the vanadyl(4)-prepulsed cells shown in (*A*), demonstrating the total (free and bound) vanadium content in these cells where the nuclear area has the highest concentration of the ion (coloured yellow). (*C*) STIM bitmap of control cells treated in the same way as in (*A*) but without addition of vanadyl(4) (cells of fig. 2A). (*D*) PIXE bitmap of cells shown in (*C*), demonstrating vanadium at trace level in random distribution.

value. However control populations subjected to similar acidification-and-recovery cycles but without vanadyl(4) addition, had similar reversals, with K^+/Na^+ ratio of 0.12 at the end of 2 h incubation. Even so, these cells always had normal DNA cell cycle profiles and continued to survive and propagate with prolonged culturing. $OH^\bullet$ is the most reactive of the oxidative free radical species[32], and capable of reacting with most biomolecules in the cell. The high reactivity of the reactive oxygen species is known to impose strict limitations on their penetration, so that unless they were released intranuclearly, it would be quite unlikely to have any direct effect on nuclear DNA. Here we demonstrated massive nuclear sequestration of vanadyl(4) ions. The oxidative reactivity in the nucleus after vanadium loading was indicated by the oxidation of the redox indicator methylene blue into the purple-coloured metachromatic oxidized state (fig. 6). Monochlorobimane-glutathione adduct fluorescence was completely abolished (total blank, not shown), in contrast to the bright fluorescence of control cells. This indicated depletion of glutathione, the principal reducing agent in

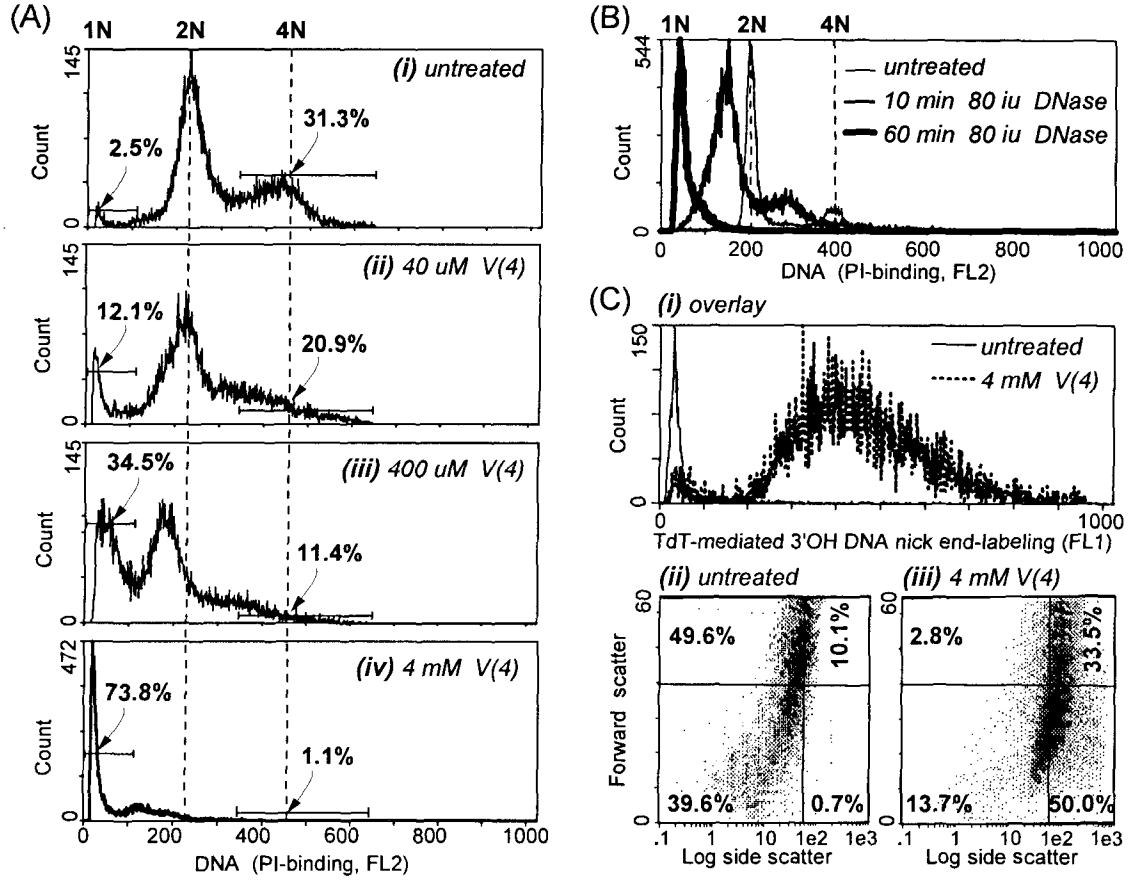

Figure 4. (*A*) Vanadyl(4) dose-response: propidium iodide (PI)-DNA binding in human Chang liver cells subjected to the acidification-and-recovery shown in figure 1. Flow cytometric evaluation. (i) Untreated cells had a 2.5% 1N DNA peak, representing the suicidal proportion in the normal proliferative cycle which had a significant 4N DNA peak. (ii) With 40 μM V(4) treatment, the suicidal proportion (1N DNA) increased nearly 5-fold to 12.1%, while the 4N DNA declined by a similar amount causing flattening of this proliferative peak. (iii) With 400 μM V(4) treatment, 1N DNA peak was augmented another 3-fold, and represents 34.5% of the total genomic DNA. (iv) With 4 mM V(4) treatment, 1N DNA represents 73.8% of total genomic DNA. (*B*) Micrococcal nuclease digestion of the control cell population where the DNase digestion had reproduced the left-shift of the DNA profile towards an eventual 1N DNA peak, as shown in (*A*), suggesting that the 1N DNA peak was fragmented DNA, shown by direct DNase digestion. (*C*) Terminal deoxynucleotidyl transferase (TdT)-mediated labeling of 3'OH ends of DNA breaks in the 4 mM vanadyl(4)-treated population showed that virtually all cells in the population had genomic DNA fragmentation. The 1N DNA peak in (*A*)iv was fragmented DNA. (ii–iii) Bitmap quartiles of flow cytometer forward- and side-scattering data where the 4 mM V(4)-treated cells showed decreased forward scattering indicating smaller surface area from downsizing, but higher side scattering indicating increased granularity, consistent with cell condensation in programmed cell death.

the cell. Abolishing the principal reducing agent of the cell added to the state of 'oxidative stress', which has recently been seen associated with the induction of cell suicide or programmed cell death[19–22]. However unlike previous demonstrations of association with reactive oxygen species that were applied extracellularly, here we have imposed direct, intranuclearly-triggered, oxidative stress via massive nuclear sequestration of vanadyl(4) and realkalinization, and demonstrated total genomic DNA destruction in virtually all cells of the population evaluated cell-by-cell in flow cytometry, in a time span of only 2 h. The rapid and total effect supported the notion that direct DNA damage is an initiator of cell suicide/programmed cell death.

Electron microscopy studies of cellular profiles after acidification with vanadyl(4) showed autophagy characterized by the presence of autophagosomes where rough endoplasmic reticulum (RER) ringed cytosolic areas to produce distinctive figure-of-eight ring configurations of RER. These and various other autophagic formations, including sequestration of mitochondria and formation of multivesicular degradative autophagosomes or autolysosomes, could be seen in the same cells (fig. 7), suggesting a strong presence of autophagic progression in these vanadium-loaded human Chang liver cells. The distinctive feature of this autophagic process is the characteristic presence of overtly rough or granulated membranes of rough endoplasmic reticulum. Although autophagy is generally perceived as involving rough endoplasmic reticulum, it has been also reported as involving the smooth parts or degranulated parts of rough endoplasmic reticulum, rather than distinctively

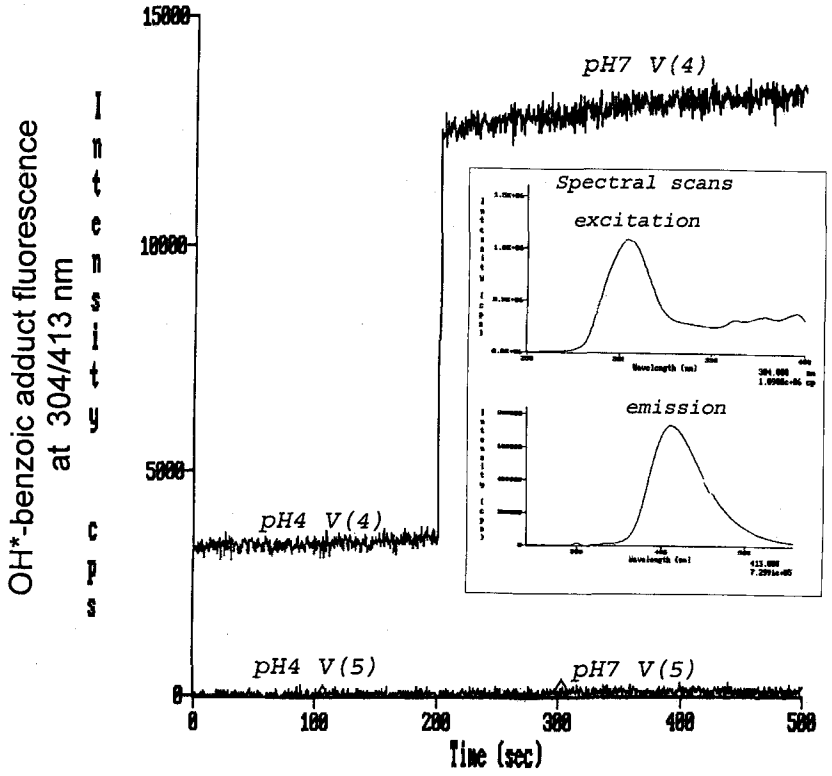

Figure 5. Spectrofluorimetric evaluation of hydroxyl free radicals generated from 4 mM vanadyl(4) at pH 4 and 7, which are equivalent to the intracellular pH of acidified and recovered cells respectively. The formation of 2-hydroxybenzoate from OH$^{\cdot}$-benzoic acid adducts was detected at excitation/emission wavelength of 304/413 nm. Inset shows the spectral scan. Specific fluorescence was 400% more at pH 7 than at pH 4. Sodium orthovanadate or metavanadate (V(5)) did not produce significant OH$^{\cdot}$ levels (base-line traces).

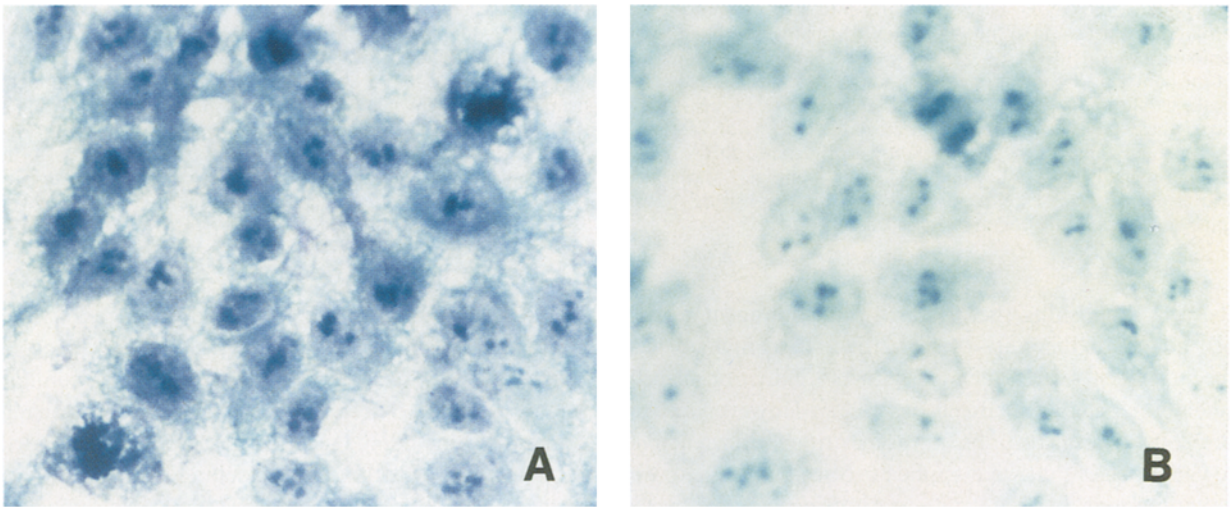

Figure 6. Methylene blue staining of human Chang liver cells (*A*) after vanadium loading (subjected to the NH_4Cl acidification for 30 min and allowed to recover for 15 min, in the presence of 4 mM vanadyl(4)), and (*B*) without vanadium loading, but similarly treated. Methylene blue is a redox indicator that turns dark or metachromatic (purple colour) when oxidized. The purple metachromatic staining in nuclei of vanadium-loaded cells in (*A*) contrasted with the overall light blue staining of control cells in (*B*). Obj. × 40.

rough parts of rough endoplasmic reticulum[33]. Autophagic digestion is not a necrotic process but a process of self-renewal that occurs in all normal living cells for the removal of effete proteins and organelles. Programmed cell death is noted for having a frequent presence of autophagic activity, in contradistinction to necrotic cell death[34]. Another distinguishing feature was the presence of intact plasma membrane in the

Figure 7. Ultrastructural profile of vanadyl(4)-treated human Chang liver cells (subjected to the NH_4Cl acidification with 4 mM vanadyl(4) for 30 min and allowed to recover for 3 min in DMEM), showing intact plasma membrane (cell margin) and various stages of autophagy in progression. Arrowhead shows characteristic figure-of-eight autophagosome formations of overtly rough-membraned rough endoplasmic reticulum (RER) in these cells. The sequestered areas in the first pair of figure-of-eight RER formation also showed small vesicles suggesting invasion by primary lysosomal vesicles that could lead to the conversion of autophagosomes into degradative autophagosome or autolysosomes as multivesiculated bodies (double-headed thick arrows). Single arrows point to mitochondria surrounded by RER in autophagosome formation. Dark lysosomal masses are seen at opposite corners of the figure. Bar = 500 nm.

vanadyl(4) loaded cells. Even with overnight 24 h incubations, the characteristic 'moth-eaten' appearance of programmed cell death merely became much more 'moth-eaten' from continued autodigestion, the plasma membrane remained distinct and intact in ultrastructural profiles. Programmed cell death is widely held to be a process of 'controlled autodigestion'[21] which is in contradistinction to necrotic cell death that is chracterized by lytic degeneration, swollen profiles and disrupted cell outlines. The ultrastructural findings supported cell death by suicide, and not by necrosis, as indicated by the cell cycle DNA profiles from flow cytometry.

Acknowledgements. We thank Mr. Chan Heng Leong for technical assistance in electron microscopy, and the National University of Singapore for funding this project.

1 Chasteen, N. D., Structure and Bonding *53* (1983) 105.
2 Carpenter, G., Biochem. Biophys. Res. Commun. *102* (1981) 1115.
3 Sit, K. H., Paramanantham, R., Bay, B. H., and Wong, K. P., Jap. J. Pharmacol. *65* (1994) 83.
4 Ishikawa, T., Trends Biochem. Sci. *17* (1992) 463.
5 Muller, M., Meijer, C., Zaman, G. J. R., Borst, P., Scheper, R. J., Mulder, N. H., de Vries, E. G. E., and Jansen, P. L. M., Proc. natl Acad. Sci. USA *91* (1994) 13033.
6 Posner, B. I., Faure, R., Burgess, J. W., Bevan, A. P., Lachance, D., Zhang-Sun, G., Fantus, I. G., Ng, J. B., Hall, D. A., Lum, B. S., and Shaver, A., J. biol. Chem. *269* (1994) 4596.
7 Thompson, H. J., Chasteen, D. N., and Meeker, L. D., Carcinogenesis *5* (1984) 849.
8 Matsumoto, J., Medical Hypothesis *43* (1994) 177.
9 French, R. J., and Jones, P. J., Life Sci. *52* (1994) 339.
10 Harland, B. F., and Harden-Williams, B. A., J. Am. Diet. Assoc. *94* (1994) 891.
11 Sit, K. H., Bay, B. H., Paramanantham, R., Thong, P., and Watt, F., J. Tiss. Cult. Meth. *15* (1993) 199.
12 Landsberg, J. P., McDonald, B., and Watt, F., Nature (Lond.) *360* (1992) 65.
13 Watt, F., Orlic, I., Loh, K. K., Sow, C. H., Thong, P., Liew, S. C., Osipowicz, T., Choo, R. F., and Tang, S. M., Nucl. Instr. Meths. *B85* (1994) 708.
14 Cargnello, J. A., Powell, J. J., Thompson, R. P. H., Crocker, P. R., and Watt, F., Analyst *120* (1995) 783.
15 Hamada, T., Experientia *15* (1994) 49.
16 Monteiro, H. P., Winterbourn, C. C., and Stern, A., Free Radic. Res. Commun. *12–13* (1991) 125.
17 Keller, R. J., Sharma, R. P., Grover, T. A., and Piette, L. H., Archs Biochem. Biophys. *265* (1988) 524.
18 Liochev, S. I., and Fridovich, I., Archs Biochem. Biophys. *29* (1991) 379.
19 Kane, D. J., Sarafian, T. A., Anton, R., Hahn, H., Gralla, E. B., Valentine, J. S., Ord, T., and Bredesen, D. E., Science *262* (1993) 1274.
20 Hockenbery, D. M., Oltvai, Z. N., Yin, X.-M., Milliman, C. L., and Korsmeyer, S. J., Cell *75* (1993) 241.
21 Thompson, C., Science *267* (1995) 1456.
22 Korsmeyer, S. J., Trends Genetics *11* (1995) 101.
23 Hansard, S. L., Ammerman, C. B., Henry, P. R., and Simpson, C. F., J. Anim. Sci. *55* (1982) 344.
24 Wei, C., Al Bayati, M. A., Culbertson, M. R., Rosenblatt, L. S., and Hansen, L. D., J. Toxicol. Environ. Health *10* (1982) 673.
25 Lee, K. P., and Gillies, P. J., Environ. Res. *40* (1986) 115.
26 Sit, K. H., and Wong, K. P., Tissue Cell *21* (1989) 321.
27 Sit, K. H., Paramanantham, R., Bay, B. H., and Wong, K. P., Anat. Rec. *240* (1994) 456.
28 Baker, M. S., and Gebicki, J. M., Archs Biochem. Biophys. *234* (1984) 258.
29 Telford, W. G., King, L. E., and Fraker, P. J., Cytometry *13* (1992) 137.
30 Umansky, S. R., in: Apoptosis: The Molecular Basis of Cell Death (Current Communications in Cell and Molecular Biology, 3), p. 193. Eds D. D. Tomei and F. O. Cope. Cold Spring Harbor Laboratory Press, New York 1991.
31 Telford, W. G., King, L. E., and Fraker, P. J., J. Immun. Meth. *172* (1994) 1.
32 Halliwell, B., and Gutteridge, J. M. C., Biochem. J. *219* (1984) 1.
33 Dunn, W. A. Jr., J. Cell Biol. *110* (1990) 1935.
34 Lockshin, R. A., and Zakeri, Z., in: Apoptosis: The Molecular Basis of Cell Death (Current Communications in Cell and Molecular Biology, 3), p. 47. Eds D. D. Tomei and F. O. Cope. Cold Spring Harbor Laboratory Press, New York 1991.